Chinese Chemical Letters 36 (2025) 110118

Contents lists available at ScienceDirect

Chinese Chemical Letters

journal homepage: www.elsevier.com/locate/cclet

The study of antibacterial activity of cationic poly(β-amino ester) regulating by amphiphilic balance

Chong Liu[a,b,d], Ling Li[a,d], Jiahui Gao[b], Yanwei Li[a,*], Nazhen Zhang[a], Jing Zang[b], Cong Liu[c], Zhaopei Guo[d], Yanhui Li[a,b,*], Huayu Tian[c,d,*]

[a] School of Materials Science and Engineering, Changchun University of Science and Technology, Changchun 130022, China
[b] School of Materials Science and Engineering, Xiamen University of Technology, Xiamen 361024, China
[c] College of Chemistry and Chemical Engineering, Xiamen University, Xiamen 361005, China
[d] Key Laboratory of Polymer Ecomaterials, Changchun Institute of Applied Chemistry, Chinese Academy of Sciences, Changchun 130022, China

ARTICLE INFO

Article history:
Received 27 January 2024
Revised 10 June 2024
Accepted 12 June 2024
Available online 13 June 2024

Keywords:
Antimicrobial
Cationic polymers
Poly(β-amino ester)s
Michael addition polymerization
Amphiphilic balance

ABSTRACT

It is well known that cationic polymers have excellent antimicrobial capacity accompanied with high biotoxicity, to reduce biotoxicity needs to decrease the number of cationic groups on polymers, which will influence antimicrobial activity. It is necessary to design a cationic polymer mimic natural antimicrobial peptide with excellent antibacterial activity and low toxicity to solve the above dilemma. Here, we designed and prepared a series of cationic poly(β-amino ester)s (PBAEs) with different cationic contents, and introducing hydrophobic alkyl chain to adjust the balance between antimicrobial activity and biotoxicity to obtain an ideal antimicrobial polymer. The optimum one of synthesized PBAE (hydrophilic cationic monomer:hydrophobic monomer = 5:5) was screened by testing cytotoxicity and minimum inhibitory concentration (MIC), which can effectively kill *S. aureus* and *E. coli* with PBAE concentration of 15 μg/mL by a spread plate bacteriostatic method and dead and alive staining test. The way of PBAE killing bacterial was destroying the membrane like natural antimicrobial peptide observed by scanning electron microscopy (SEM). In addition, PBAE did not exhibit hemolysis and cytotoxicity. In particular, from the result of animal tests, the PBAE was able to promote healing of infected wounds from removing mature *S. aureus* and *E. coli* on the surface of infected wound. As a result, our work offers a viable approach for designing antimicrobial materials, highlighting the significant potential of PBAE polymers in the field of biomedical materials.

Every year, millions of people around the world die from bacterial infections. At present, the most effective way to resolve bacterial infections is still relay on antibiotics [1]. But the overuse of antibiotics over the past decades has led to the emergence of drug-resistant bacteria, which has developed into a serious global health problem [2,3]. In order to solve this problem, researchers are enthusiastically developing antibacterial strategies to avoid drug resistance, using antibacterial materials except for antibiotics to fight bacteria, commonly used include metal ions (Ag, Cu) metal oxides (Al_2O_3, TiO_2), organic molecules (guanidinium salts, halogens, porphyrin-type photosensitizers) and antimicrobial peptides (AMPs) [4-9]. Metal ions are the oldest used bactericide with a long validity antibacterial period and good antibacterial efficiency, but the high cost and high toxicity as well as easy to produce heavy metal deposition and difficult to metabolize limit its application in body [10,11]. Some metal oxides and organic photosensitizers are semiconductor and can adsorb light of a particular wavelength to produce ROS (reactive oxygen species) to achieve photodynamic antimicrobials, but the light-dependence limits their antimicrobial application in deep tissues and organs in body [12]. Organic small molecule antimicrobials are trapped by their own toxicity and instability and not an ideal one in practical use [13]. Among these antimicrobial materials, AMPs are produced from the living body organisms themselves with safety and non-toxicity, wide antimicrobial spectrum, good stability and low bactericidal concentration [14,15]. While the source of natural AMPs was limited, and AMPs are difficult to extract, resulting in low yield and high cost, which influence the large scales application in anti-infection [16,17]. Therefore, it is important to find a kind of easy-to-obtain antibacterial materials that can simulate the antimicrobial mechanism of AMPs [18]. Synthetic polymer antibacterial materials are the primary candidate to simulate AMPs due to their

* Corresponding authors.
E-mail addresses: liyanwei@cust.edu.cn (Y. Li), lyh2008@cust.edu.cn (Y. Li), thy@ciac.ac.cn (H. Tian).

https://doi.org/10.1016/j.cclet.2024.110118
1001-8417/

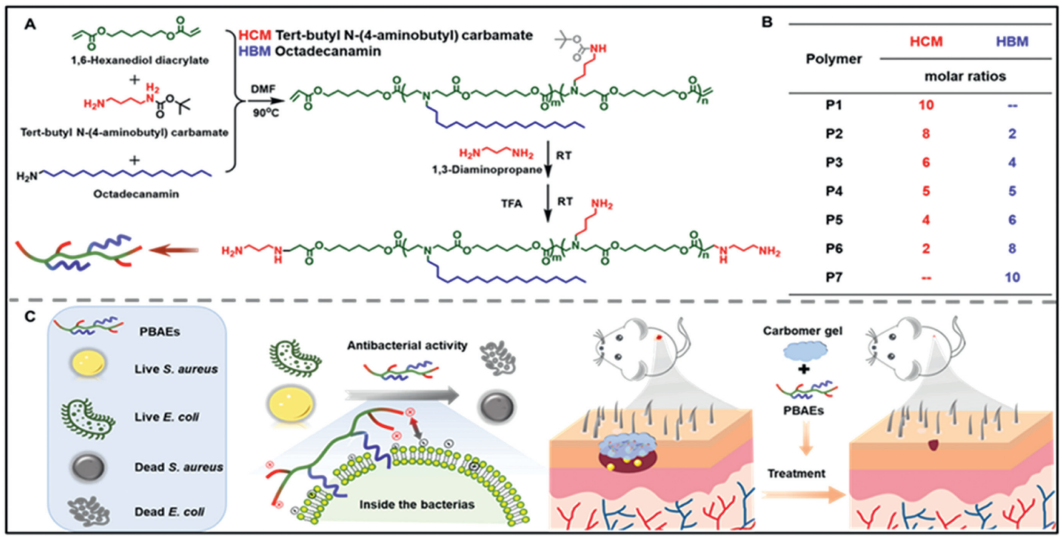

Scheme 1. PBAEs synthesis and antibacterial mechanism. (A) PBAEs were synthesized by the Michael addition reaction with different HC and HB part. (B) The proportion of subunits (HCM:HBM) of the PBAEs with the ratio of HC to HB, from 0% to 100%. (C) Antibacterial.

designable structure and low cost, which can not only obtain excellent antibacterial properties and low toxicity through structural modification, but also have wide range of options. In addition, synthetic polymers are not come from animal, so which are not immunogenic. Once a synthetic antibacterial polymer has a suitable structure and can be synthesized with stable route, it is easy to promote the use in practical application [19].

In various types of synthetic polymers, poly(β-amino ester) (PBAE) is a kind of cationic polymer and the most promising one to mimic natural AMPs, which contains a large number of amino and ester bonds in molecular chain [20,21]. The molecular structure of PBAEs can be manipulated to possess excellent biocompatibility, biodegradability, antibacterial activity and even responsiveness, which make PBAEs attract great attention in the biomedical field in recent years [22-24]. A lot of research works have been carried out the studying of PBAE in the field of, for example, anticancer drugs, antimicrobial agents, protein delivery and so on. The monomers of synthetic PBAE can be selected from a wide range of options, and the key factor for the tunability of PBAE properties is the combination of different monomers to generate different structures with the diversity of properties, and further to realize the potential of their application in the antimicrobial field [25-27]. Our molecular design is inspired by AMPs, and optimal amphiphilicity (hydrophilic/hydrophobic balance) has been identified as a key parameter for the design of antimicrobial polymers mimicking AMPs [28,29]. The presence of a cationic charge ensures selective interaction with negatively charged bacterial membranes on amphiphilic mammalian membranes, and hydrophobicity is also necessary to achieve high selectivity to bacterial cells [30].

In this study, we designed and synthesized a series of amphiphilic PBAEs consisting of cationic and hydrophobic alkyl chains (Scheme 1). In polymerization of PBAEs, *tert*-butyl *N*-(4-aminobutyl)carbamate, hexane-1,6-diyl diacrylate, and octadecanamine were used as monomers, where *tert*-butyl *N*-(4-aminobutyl)carbamate provided the hydrophilic cationic part (HC) and octadecanamine as the hydrophobic monomer (HBM), by optimizing the amphiphilic balance through adjusting the ratio of hydrophilic cationic monomer (HCM) to HBM during the Michael addition polymerization, PBAE with the better antibacterial activity and low cytotoxicity can be achieved [31]. In order to investigate the antibacterial mechanism of PBAEs, we first selected the optimum PBAE as antibacterial material to annihilate bacteria, and then scanning electron microscopy (SEM) imaging was applied

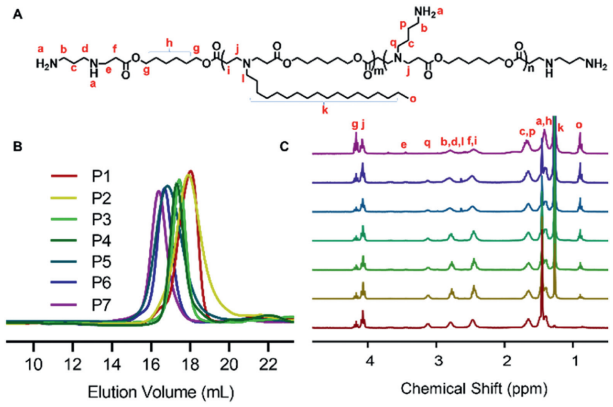

Fig. 1. Structure of PBAEs (A). GPC (B) and ^{1}H NMR (C) characterization of PBAEs.

to observe whether the bactericidal mode was similar to that of AMPs, which crumpled the bacterial membranes and disrupted the structure of bacterial membranes. To further verify the biosafety of synthetic PBAEs, we performed hemolysis experiments using rat red blood cells. Finally, we explored the antimicrobial activity of PBAEs *in vivo* through animal experiments to determine that manipulating the structure of PBAEs can yield excellent antimicrobial materials, which can effectively kill bacteria without harming normal cells and have great potential for practical application.

Firstly, we designed and prepared PBAEs by Michael addition polymerization with different ratios of HC and hydrophobic part (HB) with brush structure (Fig. 1A). All the prepared PBAEs were successfully polymerized by the result of gel permeation chromatography (GPC) with only one peak in each PBAE (Fig. 1B). The molecular weight including number-average molecular weight (M_n) and weight-average molecular weight (M_w) of PBAEs (P1–P7) were obtained and listed in Table 1 with narrow disperse (polymer dispersity index (PDI) = 1.10–1.22). Fig. 1C and Figs. S1–S7 (Supporting information) showed the ^{1}H NMR spectra of PBAEs and the corresponding proton peaks, The characteristic peak q (3.0–3.2 ppm) corresponded to the proton peak of the methylene group in HCM, with integration areas for P1–P7 listed as follows: 11.9, 11.4, 10.2, 8.2, 5.7, 3.3, 0.9. The characteristic peak o (0.8–1.0 ppm) corresponded to the proton peak of the methyl group in HBM, with integration areas for P1–P7 listed as follows: 1.8, 7.9, 12.5, 14.2,

Table 1
M_n, M_w and PDI of PBAEs by GPC.

Polymer	GPC		
	M_n	M_w	PDI
P1	6050	7400	1.2231
P2	6630	7540	1.1373
P3	7740	9180	1.1860
P4	8970	10,530	1.1739
P5	9140	10,130	1.1081
P6	9980	11,610	1.1633
P7	11,450	13,100	1.1441

Table 2
MIC values of PBAEs.

Sample	*S. aureus* (μmol/mL)	*E. coli* (μmol/mL)
P1	15.6	15.6
P2	31.5	31.5
P3	62.5	31.5
P4	15.6	15.6
P5	31.5	31.5.6
P6	62.5	125.5
P7	>500	251.0

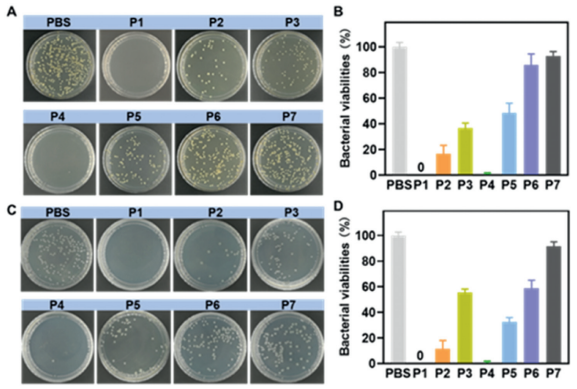

Fig. 2. Photographs of the distribution of two bacterial solid culture colonies after different cycles of co-incubation of PBAEs with (A) *S. aureus* and (C) *E. coli*. The sterilization rate of PBAEs for (B) *S. aureus* and (D) *E. coli* was calculated by colony plate counting. Data are presented as mean ± standard deviation (SD) ($n = 3$).

14.6, 10.0, 13.7. Therefore, the results of GPC and ^{1}H NMR indicated that series of PBAEs had been successfully synthesized.

In PBAEs, the HC part will bring a positive charge along the PBAEs chain to interact with anionic surface of the bacteria through electrostatic interactions, and the HB part was used to interact with the hydrophobic portion of the lipid groups in the bacterial membrane, the combination of them will annihilate bacteria effectively.

The antibacterial activity of PBAEs was determined using the minimum inhibitory concentration (MIC) with Gram-positive *S. aureus* and Gram-negative *E. coli* as the model microorganisms. The MIC values were summarized and listed in Table 2. The PBAEs with different ratios of cationic to hydrophobic alkyl groups in the solution had a great influence on the MIC values of *E. coli* and *S. aureus*. We chose the lowest MIC value of 15 μg/mL as the concentration of all materials to perform plate inhibition experiments. As shown in Figs. 2A and B, the antibacterial effect for *S. aureus* in group P1 was obvious. The livability of bacterial was 0%, while the number of colonies in groups P2 and P3 were slightly increased with the bacterial survival rate were 11.6% and 55.4%, respectively. Because the introduction of hydrophobic segments reduced the concentration of cations and thus influenced the bactericidal efficiency. However, surprisingly, the antimicrobial capacity of group P4 did not continue to reduce, where bacterial survival rate was only 0.5%, almost similar as group P1. With the continued increase of hydrophobic segments, the antimicrobial capacity continued to decrease and the bacterial survival rate was above 30%. The result suggested that the amphiphilic structure and the appropriate ratio of cationic and hydrophobic segments were the key to obtain the optimal bactericidal activity of PBAEs. We also used the same method to study antibacterial activity of PBAEs using *E. coli* as model and found a similar result (Figs. 2C and D). We hypothesized that the high bactericidal efficiency of P4 relied on the structure of P4 with appropriate proportion of HC and HB, which was easy to embed in the bacterial membrane tightly to damage the membrane of bacteria, thus showing excellent antibacterial ability.

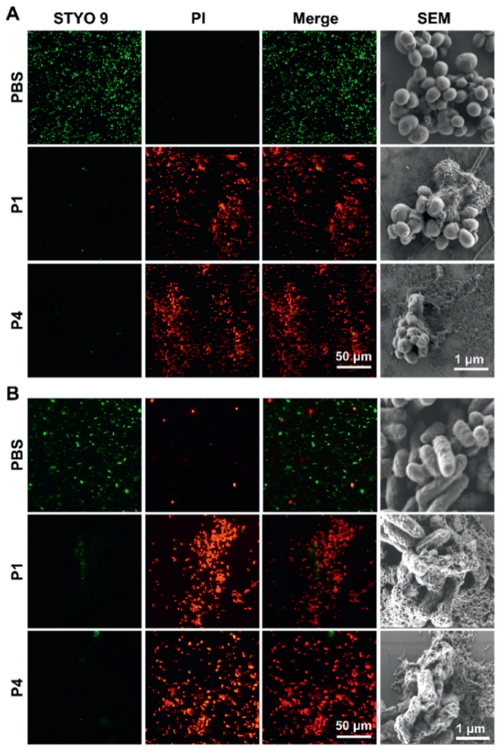

Fig. 3. Fluorescence staining images and SEM images of *S. aureus* (A) and *E. coli* (B) treated with PBS, P1 and P4.

To further investigate the antibacterial effect, *S. aureus* and *E. coli* were stained with the fluorescent dye SYTO9/PI Live and Dead Bacteria Stain Kit. PI (red) stained only the dead bacteria with damaged membrane, while SYTO9 (green) allowed access to all bacteria. As shown in Fig. 3A, most of the live *S. aureus* in the phosphate buffered saline (PBS) showed green fluorescence, and a few of them were red, indicated which had a negligible effect on the removal of bacteria. All the *S. aureus* in the P1 group showed red aureus fluorescence, and most of the *S. aureus* in the P4 group also showed a large amount of red fluorescence, which proved that P1 and P4 could kill almost all of the bacteria, further indicated that both P1 and P4 had excellent bactericidal ability. While the density of cation groups in P4 was smaller than P1, and compared with P1, P4 contained appropriate number of alkyl chains. As a result, antibacterial ability of PBAEs did not just depend on cationic part, appropriate hydrophobic structure can be an assistance. The morphological changes of Gram-positive *S. aureus* and *E. coli* after disposed by PBS, P1 and P4 were observed by SEM and showed in Fig. 3A. When *S. aureus* was treated with P1 and P4, some of *S. aureus* were destroyed into powder, and the surface of some shape retaining *S. aureus* was collapsed, indicating the damaged cell membranes of *S. aureus* were more pronounced and severe, es-

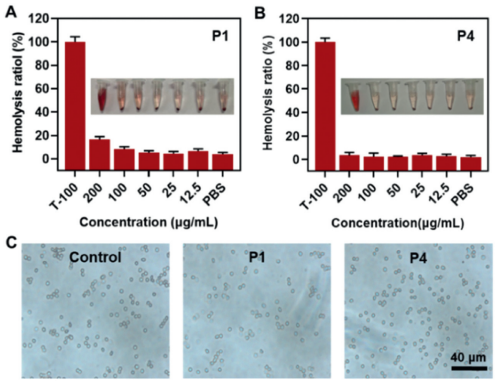

Fig. 4. Acute hemolysis experiments on P1 and P4. (A, B) Acute hemolysis test results. (C) Optical images of blood cells collected from experimental samples.

pecially for P4. While for PBS group, *S. aureus* maintained complete structure. In addition, the results of live-dead staining of *E. coli*, as shown in Fig. 3B, also revealed that P1 and P4 had a stronger killing effect, and was almost not finding living *E. coli*. The SEM images proved that the damage to *E. coli* in P1 and P4 group was more severe, and the bacterial membrane was found to be severely shrinked on the still intact *E. coli*, others collapsed into powder. These results again showed that P4 was able to kill *E. coli* by disrupt the bacterial membrane structure of the bacteria, and proper hydrophobic structure in PBAE was benefit to antibacterial.

An acute hemolysis test was used to characterize the biosafety of the prepared PBAEs (P1 and P4) (Fig. 4). In addition to normal cells, hemocompatibility is an important indicator of biosafety. Fortunately, in the acute hemolysis test, almost no erythrocytes lysis was observed when the concentration of P4 (<5%) (Fig. 4B) was high to 200 μg/mL. Only P1 showed a slight increase in hemolysis, which was maintained at about 16% at concentrations up to 200 μg/mL, as shown in Fig. 4A, perhaps due to cationic part damage the cell membrane of erythrocytes, which indicated that P1 and P4 also showed good affinity for blood cells (Fig. 4C). As a result, no obvious blood cell damage was observed in the acute hemolysis experiments, indicated P4 was safety and suitable to use in skin-friendly antibacterial field and trauma repair. The cytocompatibility of PBAEs was also assessed by testing mouse embryonic cells (NIH3T3) and mouse fibroblasts cells (L929). In Fig. S8 (Supporting information), P4 almost had no cytotoxic in the range of effective antimicrobial, suggesting that PBAEs do not have significant cytotoxic effects on normal mammalian cells. Regarding the effect of PBAEs on cell migration, cell-wound healing experiments were performed and the result was showed in Fig. S9 (Supporting information). After 24 h incubation, the scratch area of cells in all groups was significantly reduced, and scattered cells appeared in the center. After 48 h, the scratches were reduced further and some cells immigrate to the scratches and it was difficult to observe the difference between the groups with the naked eye. The above results demonstrated that P4 showed good compatibility with normal cell activity, proliferation and migration properties.

We further evaluated the *in vivo* antibacterial activity of PBAEs using a *S. aureus*-infected murine model of skin wound. All animal studies were carried out according to the guidelines approved by the Animal Welfare and Ethics Committee of Changchun Institute of Applied Chemistry, Chinese Academy of Sciences. As shown in Fig. 5A, mice received bacterial injections (*S. aureus*) on the day of surgery, and an animal model of infected wounds was successfully established. On the 10th postoperative day, wounds healed slowly in the PBS and P1 groups (Figs. 5B and C) with the percentage of residual wounds being 29.4% ± 5.7% and 16.0% ± 5.2%, respectively, while for P4 group that was low to 5.2% ± 4.4% (Fig. 5D). More-

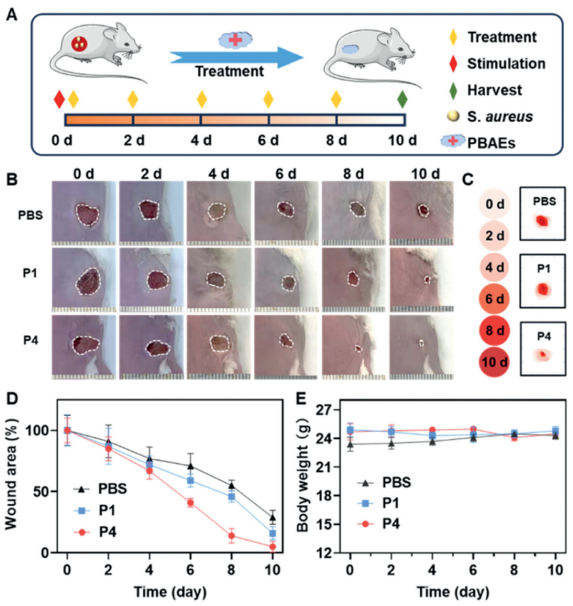

Fig. 5. Facilitating effect of P1 and P4 on the healing of back skin infected wounds in mice. (A) Schematic illustration of *S. aureus* infected wounds on the dorsal skin of mice *in vivo*. (B) Representative images of skin wounds in each group at 0, 2, 4, 6, 8, and 10 days. Only the same amount of PBS added was served as the blank control group, and PBS without nanocomposites was added to the wound with *S. aureus* stimulation as the infected control. (C, D) Changes in the sizes of wound areas of P1 or P4 and control groups. (E) Body weight changes of mice from different groups. Data are presented as mean ± SD ($n = 5$).

over, we found that the trauma was significantly reduced in the P4 group on the fourth to sixth day. The systemic toxicity of P1 and P4 was evaluated by measuring the change in body weight of mice. The results were shown in Fig. 5E. None of the mice's body weights changed significantly during treatment, indicating both of them had good biocompatibility. The systemic toxic effects of P1 and P4 on mice were observed by hematoxylin-eosin staining (H&E) staining and showed in Fig. S10 (Supporting information), indicated there were no obvious pathological damage in the hearts, livers, spleens, lungs and kidneys of mice in each group. These results suggested that P1 and P4 may accelerate wound healing by eliminating bacteria with low systemic toxicity compared with PB group. And compared with P1, the P4 group had a better wound healing effect result from (Figs. 5B–D), the result was attributed to the synergistic effect of the excellent antimicrobial capacity and superior biocompatibility of P4.

In this study, we successfully synthesized a series of amphiphilic PBAEs consisting of cationic and hydrophobic alkyl chains and screened an optimal one (P4) with good antibacterial activity and low cytotoxicity by the 5:5 ratio of HCM to HBM. The biocompatibility and low cytotoxicity of the P4 were demonstrated by *in vitro* and *in vivo* toxicity measurements. The SEM imaging observed the bactericidal mode of P4 was similar to that of AMPs, which was able to crumple the bacterial membrane and disrupt the bacterial membrane structure. Finally, the antibacterial activity of PBAEs *in vivo* was investigated by animal experiments. All the results indicated that the manipulation of the structure of PBAEs can lead to excellent antibacterial materials that can effectively kill bacteria without harming normal cells. The PBAE prepared in this study had great potential for practical applications.

Declaration of competing interest

The authors declare that they have no known competing financial interests or personal relationships that could have appeared to influence the work reported in this paper.

CRediT authorship contribution statement

Chong Liu: Writing – original draft, Data curation, Conceptualization. **Ling Li:** Resources. **Jiahui Gao:** Conceptualization. **Yanwei Li:** Funding acquisition. **Nazhen Zhang:** Resources. **Jing Zang:** Conceptualization. **Cong Liu:** Funding acquisition. **Zhaopei Guo:** Writing – review & editing. **Yanhui Li:** Writing – review & editing, Funding acquisition, Data curation, Conceptualization. **Huayu Tian:** Writing – review & editing, Supervision, Resources, Funding acquisition, Data curation, Conceptualization.

Acknowledgments

This work was financially supported by the Natural Science Foundation of Jilin Province Science and Technology Department (No. 20230101221JC), the National Natural Science Foundation of China (Nos. 52173115, 52073278, 52203189), the Research Foundation for Advanced Talents of Xiamen University of Technology (Nos. 5010423019, YKJ22052R).

Supplementary materials

Supplementary material associated with this article can be found, in the online version, at doi:10.1016/j.cclet.2024.110118.

References

[1] M.F. Moradali, B.H.A. Rehm, Nat. Rev. Microbiol. 18 (2020) 195–210.
[2] D.G.J. Larsson, C.F. Flach, Nat. Rev. Microbiol. 20 (2021) 257–269.
[3] M.T.Q. Duong, Y.S. Qin, S.H. You, J.J. Min, Exp. Mol. Med. 51 (2019) 1–15.
[4] A.Q. Zeng, R.J. Yang, Y.J. Tong, W. Zhao, Int. J. Biol. Macromol. 235 (2023) 123749.
[5] Y. Xue, L. Zhang, J.H. Zhou, et al., Adv. Funct. Mater. 34 (2023) 2308197.
[6] Z. Li, E.G. Wang, Y.Z. Zhang, et al., Nano Today 50 (2023) 101826.
[7] H.L. Zhang, Y.B. Gao, J.G. Gai, et al., J. Mater. Chem. A 6 (2018) 6442–6454.
[8] Z.L. Li, J. Chen, W. Cao, et al., Carbohydr. Polym. 180 (2018) 192–199.
[9] Y.X. Zheng, N.Y. Pan, Y. Liu, X.H. Ren, Carbohydr. Polym. 253 (2021) 117205.
[10] H. Wen, Q.H. Wu, L.Q. Liu, et al., Biomater. Sci. 11 (2023) 2870–2876.
[11] X.W. Fu, Z.Y. Yang, T. Deng, et al., J. Mater. Chem. B 8 (2020) 1481–1488.
[12] W. Shen, P. He, C.S. Xiao, X.S. Chen, Adv. Healthc. Mater. 7 (2018) 1800354.
[13] L. Rojo, L.G. Fernández, M.R. Aguilar, B.V. Lasa, Curr. Opin. Biotechnol. 76 (2022) 102752.
[14] M.E. Schafer, H. Browne, J.B. Goldberg, D.E. Greenberg, Acc. Chem. Res. 54 (2021) 2377–2385.
[15] M. Yi, T.D. Nguyen, H. Liu, et al., Adv. Funct. Mater. 33 (2023) 2213471.
[16] C.M. Nuñez, R.C. Rodríguez, C. Echeverría, M.F. García, A.M. Bonilla, Carbohydr. Polym. 302 (2023) 120438.
[17] C.C. Hanna, Y.O. Hermant, P.W.R. Harris, M.A. Brimble, Acc. Chem. Res. 54 (2021) 1878–1890.
[18] D. Ciumac, H.N. Gong, X.Z. Hu, J.R. Lu, J. Colloid. Interface Sci. 537 (2019) 163–185.
[19] Y.M. Wu, K. Chen, J.Z. Wang, et al., Prog. Polym. Sci. 141 (2023) 101679.
[20] Y.M. Qian, H.Q. Cui, R.W. Shi, et al., Eur. Polym. J. 107 (2018) 181–188.
[21] Y. Liu, Y.F. Li, D. Keskin, L.Q. Shi, Adv. Healthc. Mater. 8 (2018) 1801359.
[22] W.P. Xu, Z. Ma, G. Dhanda, J. Haldar, H.X. Xie, Chin. Chem. Lett. 34 (2023) 107847.
[23] C.F. Yang, Z.L. Xue, Y.L. Liu, et al., Mater. Sci. Eng. C 84 (2018) 254–262.
[24] H. Sun, C.P. Kabb, Y.Q. Dai, et al., Nat. Chem. 9 (2017) 817–823.
[25] F. Qi, Y.X. Qian, N. Shao, et al., ACS Appl. Mater. Interfaces 11 (2019) 18907–18913.
[26] J. Yan, L.C. Zheng, K. Hu, et al., Eur. Polym. J. 110 (2019) 41–48.
[27] A.L. Lakes, R. Peyyala, J.L. Ebersole, et al., Biomacromolecules 15 (2014) 3009–3018.
[28] Z.C. Guo, W.W. Liu, T.F. Liu, et al., Chin. Chem. Lett. 35 (2023) 109060.
[29] J. Kim, H. Yu, E. Yang, Y. Choi, P.S. Chang, LWT 174 (2023) 114421.
[30] J. Qin, J.N. Guo, Q.M. Xu, et al., ACS Appl. Mater. Interfaces 9 (2017) 10504–10511.
[31] M. Zeng, D.Z. Zhou, F. Alshehri, et al., Nano Lett. 19 (2018) 381–391.